*BABAR*-PUB-06/069
SLAC-PUB-12253
hep-ex/0612020



# Measurement of the $B^0 \to \pi^- \ell^+ \nu$ Form-Factor Shape and Branching Fraction, and Determination of $|V_{ub}|$ with a Loose Neutrino Reconstruction Technique

B. Aubert,[1] M. Bona,[1] D. Boutigny,[1] Y. Karyotakis,[1] J. P. Lees,[1] V. Poireau,[1] X. Prudent,[1] V. Tisserand,[1] A. Zghiche,[1] E. Grauges,[2] A. Palano,[3] J. C. Chen,[4] N. D. Qi,[4] G. Rong,[4] P. Wang,[4] Y. S. Zhu,[4] G. Eigen,[5] I. Ofte,[5] B. Stugu,[5] G. S. Abrams,[6] M. Battaglia,[6] D. N. Brown,[6] J. Button-Shafer,[6] R. N. Cahn,[6] Y. Groysman,[6] R. G. Jacobsen,[6] J. A. Kadyk,[6] L. T. Kerth,[6] Yu. G. Kolomensky,[6] G. Kukartsev,[6] D. Lopes Pegna,[6] G. Lynch,[6] L. M. Mir,[6] T. J. Orimoto,[6] M. Pripstein,[6] N. A. Roe,[6] M. T. Ronan,[6,*] K. Tackmann,[6] W. A. Wenzel,[6] P. del Amo Sanchez,[7] M. Barrett,[7] T. J. Harrison,[7] A. J. Hart,[7] C. M. Hawkes,[7] A. T. Watson,[7] T. Held,[8] H. Koch,[8] B. Lewandowski,[8] M. Pelizaeus,[8] K. Peters,[8] T. Schroeder,[8] M. Steinke,[8] J. T. Boyd,[9] J. P. Burke,[9] W. N. Cottingham,[9] D. Walker,[9] D. J. Asgeirsson,[10] T. Cuhadar-Donszelmann,[10] B. G. Fulsom,[10] C. Hearty,[10] N. S. Knecht,[10] T. S. Mattison,[10] J. A. McKenna,[10] A. Khan,[11] P. Kyberd,[11] M. Saleem,[11] D. J. Sherwood,[11] L. Teodorescu,[11] V. E. Blinov,[12] A. D. Bukin,[12] V. P. Druzhinin,[12] V. B. Golubev,[12] A. P. Onuchin,[12] S. I. Serednyakov,[12] Yu. I. Skovpen,[12] E. P. Solodov,[12] K. Yu Todyshev,[12] M. Bondioli,[13] M. Bruinsma,[13] M. Chao,[13] S. Curry,[13] I. Eschrich,[13] D. Kirkby,[13] A. J. Lankford,[13] P. Lund,[13] M. Mandelkern,[13] E. C. Martin,[13] D. P. Stoker,[13] S. Abachi,[14] C. Buchanan,[14] S. D. Foulkes,[15] J. W. Gary,[15] F. Liu,[15] O. Long,[15] B. C. Shen,[15] L. Zhang,[15] E. J. Hill,[16] H. P. Paar,[16] S. Rahatlou,[16] V. Sharma,[16] J. W. Berryhill,[17] C. Campagnari,[17] A. Cunha,[17] B. Dahmes,[17] T. M. Hong,[17] D. Kovalskyi,[17] J. D. Richman,[17] T. W. Beck,[18] A. M. Eisner,[18] C. J. Flacco,[18] C. A. Heusch,[18] J. Kroseberg,[18] W. S. Lockman,[18] T. Schalk,[18] B. A. Schumm,[18] A. Seiden,[18] D. C. Williams,[18] M. G. Wilson,[18] L. O. Winstrom,[18] E. Chen,[19] C. H. Cheng,[19] A. Dvoretskii,[19] F. Fang,[19] D. G. Hitlin,[19] I. Narsky,[19] T. Piatenko,[19] F. C. Porter,[19] G. Mancinelli,[20] B. T. Meadows,[20] K. Mishra,[20] M. D. Sokoloff,[20] F. Blanc,[21] P. C. Bloom,[21] S. Chen,[21] W. T. Ford,[21] J. F. Hirschauer,[21] A. Kreisel,[21] M. Nagel,[21] U. Nauenberg,[21] A. Olivas,[21] J. G. Smith,[21] K. A. Ulmer,[21] S. R. Wagner,[21] J. Zhang,[21] A. Chen,[22] E. A. Eckhart,[22] A. Soffer,[22] W. H. Toki,[22] R. J. Wilson,[22] F. Winklmeier,[22] Q. Zeng,[22] D. D. Altenburg,[23] E. Feltresi,[23] A. Hauke,[23] H. Jasper,[23] J. Merkel,[23] A. Petzold,[23] B. Spaan,[23] K. Wacker,[23] T. Brandt,[24] V. Klose,[24] H. M. Lacker,[24] W. F. Mader,[24] R. Nogowski,[24] J. Schubert,[24] K. R. Schubert,[24] R. Schwierz,[24] J. E. Sundermann,[24] A. Volk,[24] D. Bernard,[25] G. R. Bonneaud,[25] E. Latour,[25] Ch. Thiebaux,[25] M. Verderi,[25] P. J. Clark,[26] W. Gradl,[26] F. Muheim,[26] S. Playfer,[26] A. I. Robertson,[26] Y. Xie,[26] M. Andreotti,[27] D. Bettoni,[27] C. Bozzi,[27] R. Calabrese,[27] G. Cibinetto,[27] E. Luppi,[27] M. Negrini,[27] A. Petrella,[27] L. Piemontese,[27] E. Prencipe,[27] F. Anulli,[28] R. Baldini-Ferroli,[28] A. Calcaterra,[28] R. de Sangro,[28] G. Finocchiaro,[28] S. Pacetti,[28] P. Patteri,[28] I. M. Peruzzi,[28,†] M. Piccolo,[28] M. Rama,[28] A. Zallo,[28] A. Buzzo,[29] R. Contri,[29] M. Lo Vetere,[29] M. M. Macri,[29] M. R. Monge,[29] S. Passaggio,[29] C. Patrignani,[29] E. Robutti,[29] A. Santroni,[29] S. Tosi,[29] K. S. Chaisanguanthum,[30] M. Morii,[30] J. Wu,[30] R. S. Dubitzky,[31] J. Marks,[31] S. Schenk,[31] U. Uwer,[31] D. J. Bard,[32] P. D. Dauncey,[32] R. L. Flack,[32] J. A. Nash,[32] M. B. Nikolich,[32] W. Panduro Vazquez,[32] P. K. Behera,[33] X. Chai,[33] M. J. Charles,[33] U. Mallik,[33] N. T. Meyer,[33] V. Ziegler,[33] J. Cochran,[34] H. B. Crawley,[34] L. Dong,[34] V. Eyges,[34] W. T. Meyer,[34] S. Prell,[34] E. I. Rosenberg,[34] A. E. Rubin,[34] A. V. Gritsan,[35] A. G. Denig,[36] M. Fritsch,[36] G. Schott,[36] N. Arnaud,[37] M. Davier,[37] G. Grosdidier,[37] A. Höcker,[37] V. Lepeltier,[37] F. Le Diberder,[37] A. M. Lutz,[37] S. Pruvot,[37] S. Rodier,[37] P. Roudeau,[37] M. H. Schune,[37] J. Serrano,[37] A. Stocchi,[37] W. F. Wang,[37] G. Wormser,[37] D. J. Lange,[38] D. M. Wright,[38] C. A. Chavez,[39] I. J. Forster,[39] J. R. Fry,[39] E. Gabathuler,[39] R. Gamet,[39] D. E. Hutchcroft,[39] D. J. Payne,[39] K. C. Schofield,[39] C. Touramanis,[39] A. J. Bevan,[40] K. A. George,[40] F. Di Lodovico,[40] W. Menges,[40] R. Sacco,[40] G. Cowan,[41] H. U. Flaecher,[41] D. A. Hopkins,[41] P. S. Jackson,[41] T. R. McMahon,[41] F. Salvatore,[41] A. C. Wren,[41] D. N. Brown,[42] C. L. Davis,[42] J. Allison,[43] N. R. Barlow,[43] R. J. Barlow,[43] Y. M. Chia,[43] C. L. Edgar,[43] G. D. Lafferty,[43] T. J. West,[43] J. I. Yi,[43] C. Chen,[44] W. D. Hulsbergen,[44] A. Jawahery,[44] C. K. Lae,[44] D. A. Roberts,[44] G. Simi,[44] G. Blaylock,[45] C. Dallapiccola,[45] S. S. Hertzbach,[45] X. Li,[45] T. B. Moore,[45] E. Salvati,[45] S. Saremi,[45] R. Cowan,[46] G. Sciolla,[46] S. J. Sekula,[46] M. Spitznagel,[46] F. Taylor,[46] R. K. Yamamoto,[46] H. Kim,[47] S. E. Mclachlin,[47] P. M. Patel,[47] S. H. Robertson,[47] A. Lazzaro,[48] V. Lombardo,[48] F. Palombo,[48] J. M. Bauer,[49] L. Cremaldi,[49] V. Eschenburg,[49] R. Godang,[49] R. Kroeger,[49] D. A. Sanders,[49] D. J. Summers,[49] H. W. Zhao,[49] S. Brunet,[50]

D. Côté,[50] M. Simard,[50] P. Taras,[50] F. B. Viaud,[50] H. Nicholson,[51] N. Cavallo,[52,‡] G. De Nardo,[52] F. Fabozzi,[52,‡] C. Gatto,[52] L. Lista,[52] D. Monorchio,[52] P. Paolucci,[52] D. Piccolo,[52] C. Sciacca,[52] M. A. Baak,[53] G. Raven,[53] H. L. Snoek,[53] C. P. Jessop,[54] J. M. LoSecco,[54] G. Benelli,[55] L. A. Corwin,[55] K. K. Gan,[55] K. Honscheid,[55] D. Hufnagel,[55] H. Kagan,[55] R. Kass,[55] J. P. Morris,[55] A. M. Rahimi,[55] J. J. Regensburger,[55] R. Ter-Antonyan,[55] Q. K. Wong,[55] N. L. Blount,[56] J. Brau,[56] R. Frey,[56] O. Igonkina,[56] J. A. Kolb,[56] M. Lu,[56] C. T. Potter,[56] R. Rahmat,[56] N. B. Sinev,[56] D. Strom,[56] J. Strube,[56] E. Torrence,[56] A. Gaz,[57] M. Margoni,[57] M. Morandin,[57] A. Pompili,[57] M. Posocco,[57] M. Rotondo,[57] F. Simonetto,[57] R. Stroili,[57] C. Voci,[57] E. Ben-Haim,[58] H. Briand,[58] J. Chauveau,[58] P. David,[58] L. Del Buono,[58] Ch. de la Vaissière,[58] O. Hamon,[58] B. L. Hartfiel,[58] Ph. Leruste,[58] J. Malclès,[58] J. Ocariz,[58] L. Gladney,[59] M. Biasini,[60] R. Covarelli,[60] C. Angelini,[61] G. Batignani,[61] S. Bettarini,[61] G. Calderini,[61] M. Carpinelli,[61] R. Cenci,[61] F. Forti,[61] M. A. Giorgi,[61] A. Lusiani,[61] G. Marchiori,[61] M. A. Mazur,[61] M. Morganti,[61] N. Neri,[61] E. Paoloni,[61] G. Rizzo,[61] J. J. Walsh,[61] M. Haire,[62] J. Biesiada,[63] P. Elmer,[63] Y. P. Lau,[63] C. Lu,[63] J. Olsen,[63] A. J. S. Smith,[63] A. V. Telnov,[63] F. Bellini,[64] G. Cavoto,[64] A. D'Orazio,[64] D. del Re,[64] E. Di Marco,[64] R. Faccini,[64] F. Ferrarotto,[64] F. Ferroni,[64] M. Gaspero,[64] P. D. Jackson,[64] L. Li Gioi,[64] M. A. Mazzoni,[64] S. Morganti,[64] G. Piredda,[64] F. Polci,[64] C. Voena,[64] M. Ebert,[65] H. Schröder,[65] R. Waldi,[65] T. Adye,[66] G. Castelli,[66] B. Franek,[66] E. O. Olaiya,[66] S. Ricciardi,[66] W. Roethel,[66] F. F. Wilson,[66] R. Aleksan,[67] S. Emery,[67] M. Escalier,[67] A. Gaidot,[67] S. F. Ganzhur,[67] G. Hamel de Monchenault,[67] W. Kozanecki,[67] M. Legendre,[67] G. Vasseur,[67] Ch. Yèche,[67] M. Zito,[67] X. R. Chen,[68] H. Liu,[68] W. Park,[68] M. V. Purohit,[68] J. R. Wilson,[68] M. T. Allen,[69] D. Aston,[69] R. Bartoldus,[69] P. Bechtle,[69] N. Berger,[69] R. Claus,[69] J. P. Coleman,[69] M. R. Convery,[69] J. C. Dingfelder,[69] J. Dorfan,[69] G. P. Dubois-Felsmann,[69] D. Dujmic,[69] W. Dunwoodie,[69] R. C. Field,[69] T. Glanzman,[69] S. J. Gowdy,[69] M. T. Graham,[69] P. Grenier,[69] V. Halyo,[69] C. Hast,[69] T. Hryn'ova,[69] W. R. Innes,[69] M. H. Kelsey,[69] P. Kim,[69] D. W. G. S. Leith,[69] S. Li,[69] S. Luitz,[69] V. Luth,[69] H. L. Lynch,[69] D. B. MacFarlane,[69] H. Marsiske,[69] R. Messner,[69] D. R. Muller,[69] C. P. O'Grady,[69] V. E. Ozcan,[69] A. Perazzo,[69] M. Perl,[69] T. Pulliam,[69] B. N. Ratcliff,[69] A. Roodman,[69] A. A. Salnikov,[69] R. H. Schindler,[69] J. Schwiening,[69] A. Snyder,[69] J. Stelzer,[69] D. Su,[69] M. K. Sullivan,[69] K. Suzuki,[69] S. K. Swain,[69] J. M. Thompson,[69] J. Va'vra,[69] N. van Bakel,[69] A. P. Wagner,[69] M. Weaver,[69] W. J. Wisniewski,[69] M. Wittgen,[69] D. H. Wright,[69] H. W. Wulsin,[69] A. K. Yarritu,[69] K. Yi,[69] C. C. Young,[69] P. R. Burchat,[70] A. J. Edwards,[70] S. A. Majewski,[70] B. A. Petersen,[70] L. Wilden,[70] S. Ahmed,[71] M. S. Alam,[71] R. Bula,[71] J. A. Ernst,[71] V. Jain,[71] B. Pan,[71] M. A. Saeed,[71] F. R. Wappler,[71] S. B. Zain,[71] W. Bugg,[72] M. Krishnamurthy,[72] S. M. Spanier,[72] R. Eckmann,[73] J. L. Ritchie,[73] C. J. Schilling,[73] R. F. Schwitters,[73] J. M. Izen,[74] X. C. Lou,[74] S. Ye,[74] F. Bianchi,[75] F. Gallo,[75] D. Gamba,[75] M. Pelliccioni,[75] M. Bomben,[76] L. Bosisio,[76] C. Cartaro,[76] F. Cossutti,[76] G. Della Ricca,[76] L. Lanceri,[76] L. Vitale,[76] V. Azzolini,[77] N. Lopez-March,[77] F. Martinez-Vidal,[77] A. Oyanguren,[77] J. Albert,[78] Sw. Banerjee,[78] B. Bhuyan,[78] K. Hamano,[78] R. Kowalewski,[78] I. M. Nugent,[78] J. M. Roney,[78] R. J. Sobie,[78] J. J. Back,[79] P. F. Harrison,[79] T. E. Latham,[79] G. B. Mohanty,[79] M. Pappagallo,[79,§] H. R. Band,[80] X. Chen,[80] S. Dasu,[80] K. T. Flood,[80] J. J. Hollar,[80] P. E. Kutter,[80] B. Mellado,[80] Y. Pan,[80] M. Pierini,[80] R. Prepost,[80] S. L. Wu,[80] Z. Yu,[80] and H. Neal[81]

(The *BABAR* Collaboration)

[1]*Laboratoire de Physique des Particules, IN2P3/CNRS et Université de Savoie, F-74941 Annecy-Le-Vieux, France*
[2]*Universitat de Barcelona, Facultat de Fisica, Departament ECM, E-08028 Barcelona, Spain*
[3]*Università di Bari, Dipartimento di Fisica and INFN, I-70126 Bari, Italy*
[4]*Institute of High Energy Physics, Beijing 100039, China*
[5]*University of Bergen, Institute of Physics, N-5007 Bergen, Norway*
[6]*Lawrence Berkeley National Laboratory and University of California, Berkeley, California 94720, USA*
[7]*University of Birmingham, Birmingham, B15 2TT, United Kingdom*
[8]*Ruhr Universität Bochum, Institut für Experimentalphysik 1, D-44780 Bochum, Germany*
[9]*University of Bristol, Bristol BS8 1TL, United Kingdom*
[10]*University of British Columbia, Vancouver, British Columbia, Canada V6T 1Z1*
[11]*Brunel University, Uxbridge, Middlesex UB8 3PH, United Kingdom*
[12]*Budker Institute of Nuclear Physics, Novosibirsk 630090, Russia*
[13]*University of California at Irvine, Irvine, California 92697, USA*
[14]*University of California at Los Angeles, Los Angeles, California 90024, USA*
[15]*University of California at Riverside, Riverside, California 92521, USA*
[16]*University of California at San Diego, La Jolla, California 92093, USA*
[17]*University of California at Santa Barbara, Santa Barbara, California 93106, USA*
[18]*University of California at Santa Cruz, Institute for Particle Physics, Santa Cruz, California 95064, USA*
[19]*California Institute of Technology, Pasadena, California 91125, USA*
[20]*University of Cincinnati, Cincinnati, Ohio 45221, USA*

[21] University of Colorado, Boulder, Colorado 80309, USA
[22] Colorado State University, Fort Collins, Colorado 80523, USA
[23] Universität Dortmund, Institut für Physik, D-44221 Dortmund, Germany
[24] Technische Universität Dresden, Institut für Kern- und Teilchenphysik, D-01062 Dresden, Germany
[25] Laboratoire Leprince-Ringuet, CNRS/IN2P3, Ecole Polytechnique, F-91128 Palaiseau, France
[26] University of Edinburgh, Edinburgh EH9 3JZ, United Kingdom
[27] Università di Ferrara, Dipartimento di Fisica and INFN, I-44100 Ferrara, Italy
[28] Laboratori Nazionali di Frascati dell'INFN, I-00044 Frascati, Italy
[29] Università di Genova, Dipartimento di Fisica and INFN, I-16146 Genova, Italy
[30] Harvard University, Cambridge, Massachusetts 02138, USA
[31] Universität Heidelberg, Physikalisches Institut, Philosophenweg 12, D-69120 Heidelberg, Germany
[32] Imperial College London, London, SW7 2AZ, United Kingdom
[33] University of Iowa, Iowa City, Iowa 52242, USA
[34] Iowa State University, Ames, Iowa 50011-3160, USA
[35] Johns Hopkins University, Baltimore, Maryland 21218, USA
[36] Universität Karlsruhe, Institut für Experimentelle Kernphysik, D-76021 Karlsruhe, Germany
[37] Laboratoire de l'Accélérateur Linéaire, IN2P3/CNRS et Université Paris-Sud 11,
Centre Scientifique d'Orsay, B. P. 34, F-91898 ORSAY Cedex, France
[38] Lawrence Livermore National Laboratory, Livermore, California 94550, USA
[39] University of Liverpool, Liverpool L69 7ZE, United Kingdom
[40] Queen Mary, University of London, E1 4NS, United Kingdom
[41] University of London, Royal Holloway and Bedford New College, Egham, Surrey TW20 0EX, United Kingdom
[42] University of Louisville, Louisville, Kentucky 40292, USA
[43] University of Manchester, Manchester M13 9PL, United Kingdom
[44] University of Maryland, College Park, Maryland 20742, USA
[45] University of Massachusetts, Amherst, Massachusetts 01003, USA
[46] Massachusetts Institute of Technology, Laboratory for Nuclear Science, Cambridge, Massachusetts 02139, USA
[47] McGill University, Montréal, Québec, Canada H3A 2T8
[48] Università di Milano, Dipartimento di Fisica and INFN, I-20133 Milano, Italy
[49] University of Mississippi, University, Mississippi 38677, USA
[50] Université de Montréal, Physique des Particules, Montréal, Québec, Canada H3C 3J7
[51] Mount Holyoke College, South Hadley, Massachusetts 01075, USA
[52] Università di Napoli Federico II, Dipartimento di Scienze Fisiche and INFN, I-80126, Napoli, Italy
[53] NIKHEF, National Institute for Nuclear Physics and High Energy Physics, NL-1009 DB Amsterdam, The Netherlands
[54] University of Notre Dame, Notre Dame, Indiana 46556, USA
[55] Ohio State University, Columbus, Ohio 43210, USA
[56] University of Oregon, Eugene, Oregon 97403, USA
[57] Università di Padova, Dipartimento di Fisica and INFN, I-35131 Padova, Italy
[58] Laboratoire de Physique Nucléaire et de Hautes Energies,
IN2P3/CNRS, Université Pierre et Marie Curie-Paris6,
Université Denis Diderot-Paris7, F-75252 Paris, France
[59] University of Pennsylvania, Philadelphia, Pennsylvania 19104, USA
[60] Università di Perugia, Dipartimento di Fisica and INFN, I-06100 Perugia, Italy
[61] Università di Pisa, Dipartimento di Fisica, Scuola Normale Superiore and INFN, I-56127 Pisa, Italy
[62] Prairie View A&M University, Prairie View, Texas 77446, USA
[63] Princeton University, Princeton, New Jersey 08544, USA
[64] Università di Roma La Sapienza, Dipartimento di Fisica and INFN, I-00185 Roma, Italy
[65] Universität Rostock, D-18051 Rostock, Germany
[66] Rutherford Appleton Laboratory, Chilton, Didcot, Oxon, OX11 0QX, United Kingdom
[67] DSM/Dapnia, CEA/Saclay, F-91191 Gif-sur-Yvette, France
[68] University of South Carolina, Columbia, South Carolina 29208, USA
[69] Stanford Linear Accelerator Center, Stanford, California 94309, USA
[70] Stanford University, Stanford, California 94305-4060, USA
[71] State University of New York, Albany, New York 12222, USA
[72] University of Tennessee, Knoxville, Tennessee 37996, USA
[73] University of Texas at Austin, Austin, Texas 78712, USA
[74] University of Texas at Dallas, Richardson, Texas 75083, USA
[75] Università di Torino, Dipartimento di Fisica Sperimentale and INFN, I-10125 Torino, Italy
[76] Università di Trieste, Dipartimento di Fisica and INFN, I-34127 Trieste, Italy
[77] IFIC, Universitat de Valencia-CSIC, E-46071 Valencia, Spain
[78] University of Victoria, Victoria, British Columbia, Canada V8W 3P6
[79] Department of Physics, University of Warwick, Coventry CV4 7AL, United Kingdom
[80] University of Wisconsin, Madison, Wisconsin 53706, USA
[81] Yale University, New Haven, Connecticut 06511, USA

(Dated: December 12, 2006)

We report the results of a study of the exclusive charmless semileptonic decay, $B^0 \to \pi^-\ell^+\nu$, undertaken with approximately 227 million $B\overline{B}$ pairs collected at the $\Upsilon(4S)$ resonance with the *BABAR* detector. The analysis uses events in which the signal $B$ decays are reconstructed with an innovative loose neutrino reconstruction technique. We obtain partial branching fractions in 12 bins of $q^2$, the momentum transfer squared, from which we extract the $f_+(q^2)$ form-factor shape and the total branching fraction $\mathcal{B}(B^0 \to \pi^-\ell^+\nu) = (1.46 \pm 0.07_{stat} \pm 0.08_{syst}) \times 10^{-4}$. Based on a recent unquenched lattice QCD calculation of the form factor in the range $q^2 > 16$ GeV$^2$, we find the magnitude of the CKM matrix element $|V_{ub}|$ to be $\left(4.1 \pm 0.2_{stat} \pm 0.2_{syst}{}^{+0.6}_{-0.4\,\mathrm{FF}}\right) \times 10^{-3}$, where the last uncertainty is due to the normalization of the form factor.

PACS numbers: 13.20.He, 12.15.Hh, 12.38.Qk, 14.40.Nd

A precise measurement of $|V_{ub}|$, the smallest element of the CKM matrix [1], will constrain the description of weak interactions and *CP* violation in the Standard Model. The rate for exclusive $B^0 \to \pi^-\ell^+\nu$ decays [2] is proportional to $|V_{ub}f_+(q^2)|^2$, where the form factor $f_+(q^2)$ depends on $q^2$, the momentum transfer squared. Values of $f_+(q^2)$ for $B^0 \to \pi^-\ell^+\nu$ decays are provided by unquenched lattice QCD (LQCD) calculations (HPQCD [3], FNAL [4]), presently reliable only at large $q^2$ ($> 16$ GeV$^2$), by light cone sum rules (LCSR) calculations [5], based on approximations only valid at small $q^2$ ($< 16$ GeV$^2$), and by the ISGW2 quark model calculations [6]. Uncertainties on these calculations dominate the errors on the computed values of $|V_{ub}|$. The QCD theoretical predictions are at present more precise for $B^0 \to \pi^-\ell^+\nu$ than for other exclusive $B \to X_u\ell\nu$ decays, where $X_u$ stands for any charmless meson. Experimental data can be used to discriminate between the various calculations by precisely measuring the $f_+(q^2)$ shape, thereby leading to a smaller theoretical uncertainty on $|V_{ub}|$.

Values of $|V_{ub}|$ have previously been extracted from $B^0 \to \pi^-\ell^+\nu$ measurements by CLEO [7], *BABAR* [8, 9] and Belle [10]. In this letter, we present measurements of the partial branching fractions (BF) $\Delta\mathcal{B}(B^0 \to \pi^-\ell^+\nu, q^2)$ in 12 bins of $q^2$ using an innovative loose neutrino reconstruction technique. This leads to more precise values of the total BF $\mathcal{B}(B^0 \to \pi^-\ell^+\nu)$ and of the $f_+(q^2)$ form-factor shape, which supersede those of our previous untagged measurement [8]. We combine the values of $\Delta\mathcal{B}(q^2)$ with recent form-factor calculations [3, 4, 5] to obtain a value of $|V_{ub}|$.

The data set used in this analysis contains approximately 227 million $B\overline{B}$ pairs corresponding to an integrated luminosity of 206 fb$^{-1}$ collected at the $\Upsilon(4S)$ resonance with the *BABAR* detector [11] at the PEP-II asymmetric-energy $e^+e^-$ collider, and of 27.0 fb$^{-1}$ integrated luminosity of data collected approximately 40 MeV below the $\Upsilon(4S)$ resonance (denoted "off-resonance data"). To estimate the signal efficiency, and the signal and background distributions, we use a detailed Monte Carlo (MC) simulation of generic $B\overline{B}$ and $u\overline{u}/d\overline{d}/s\overline{s}/c\overline{c}/\tau^+\tau^-$ "continuum" events as well as $B^0 \to \pi^-\ell^+\nu$ signal events. Signal MC events are produced by the FLATQ2 generator [12] and are reweighted to reproduce the Becirevic-Kaidalov (BK) parametrization [13] of $f_+(q^2, \alpha, c_B)$ where the values of the shape and normalization parameters, $\alpha$ and $c_B$, are taken from Ref. [8].

We reconstruct $B$ meson candidates using $\pi^\pm$ and $\ell^\mp$ tracks together with the event's missing momentum $\vec{p}_{miss}$ as an approximation to the signal neutrino momentum. The decay of the second $B$ meson is not explicitly reconstructed. The neutrino four-momentum $P_{miss} \equiv (|\vec{p}_{miss}|, \vec{p}_{miss})$ is inferred from the difference between the momentum of the colliding-beam particles $\vec{p}_{beams}$, and the sum of the momenta of all the charged and neutral particles detected in a single event $\vec{p}_{tot}$, such that $\vec{p}_{miss} \equiv \vec{p}_{beams} - \vec{p}_{tot}$. Compared with the tagged analyses in which the two $B$ mesons are explicitly reconstructed [9, 10], the neutrino reconstruction approach yields a lower signal purity but a significant increase in the signal reconstruction efficiency. The present loose neutrino reconstruction technique also increases the signal efficiency substantially with respect to the previous untagged approach by avoiding the tight neutrino quality cuts [7, 8] which ensure that the neutrino properties are well taken into account when computing $q^2 = (P_\ell + P_\nu)^2$. In this analysis, we calculate instead the momentum transfer as $q^2 = (P_B - P_\pi)^2$, where the ambiguity in the direction of the $B$ meson is handled by use of the method described in Ref. [14]. In this way, the value of $q^2$ is unaffected by any mis-reconstruction of the rest of the event. We obtain a $q^2$ resolution of $\sigma = 0.52$ GeV$^2$ for the signal candidates in which the pion candidate track truly comes from a $B^0 \to \pi^-\ell^+\nu$ decay (91% of the total). We correct for the reconstruction effects on the $q^2$ resolution by applying an unregularized unfolding algorithm to the measured $q^2$ spectrum [15].

To separate the $B^0 \to \pi^-\ell^+\nu$ signal from the backgrounds, we require two well-reconstructed tracks associated with a lepton-pion pair. The electron (muon) tracks are required to have momenta greater than 0.5 (1.0) GeV in the laboratory frame to avoid misidentified leptons and secondary semileptonic decays. We ensure that the momenta of the lepton and pion candidates are

kinematically compatible with a real $B^0 \to \pi^-\ell^+\nu$ decay. This requires that a geometrical vertex fit of the two charged tracks gives a $\chi^2$ probability greater than 0.01 and that the angle between the $Y$ and $B$ momenta in the $\Upsilon(4S)$ frame takes a physical value: $|\cos\theta_{BY}| < 1$, where the pseudo-particle $Y$ is defined by its four-momentum $P_Y \equiv (P_\pi + P_\ell)$. Most backgrounds are efficiently rejected by $q^2$-dependent cuts on the helicity angle $\theta_\ell$ of the $W$ boson [12], on the angle between the thrust axes of the $Y$ and of the rest of the event, on the polar angle associated with $\vec{p}_{miss}$, and on the squared invariant mass of $P_{miss}$. We reject $B^0 \to \pi^-\mu^+\nu$ candidates with $Y$ mass close to the $J/\psi$ mass to avoid $J/\psi \to \mu^+\mu^-$ decays. Non-$B\overline{B}$ events are suppressed by requiring the ratio of second to zeroth Fox-Wolfram moments to be smaller than 0.5, and by cuts [16] on the number of tracks and clusters. Radiative Bhabha and two-photon processes are rejected by vetoing events containing a photon conversion and by requiring $(\vec{p}_{tot}\cdot\hat{z})/E_{tot} < 0.64$ and $(\vec{p}_{tot}\cdot\hat{z})/E_{tot} > 0.35$ for candidates in the electron and positron channels, respectively, where the $z$ axis is given by the electron beam direction. We reduce the remaining backgrounds with the variables $\Delta E = (\vec{p}_B\cdot\vec{p}_{beams} - s/2)/\sqrt{s}$ and $m_{ES} = \sqrt{(s/2 + \vec{p}_B\cdot\vec{p}_{beams})^2/E^2_{beams} - \vec{p}^{\,2}_B}$, where $\vec{p}_B = \vec{p}_\pi + \vec{p}_\ell + \vec{p}_{miss}$ and $\sqrt{s}$ is the total energy in the $\Upsilon(4S)$ frame. Only candidates with $|\Delta E| < 1.0$ GeV and $m_{ES} > 5.19$ GeV are retained. When several candidates remain in an event after these cuts, the candidate with $\cos\theta_\ell$ closest to zero is selected. This rejects 30% of the combinatorial signal candidates while keeping 97% of the correct ones. The signal event reconstruction efficiency varies between 6.7% and 9.8%, depending on the $q^2$ bin.

The $B^0 \to \pi^-\ell^+\nu$ signal yield is obtained as a function of $q^2$ by performing a two-dimensional extended maximum-likelihood fit [17] on $m_{\rm ES}$, and $\Delta E$ in each bin of $q^2$. The data samples in each $q^2$ bin are divided into four categories: $B^0 \to \pi^-\ell^+\nu$ signal, other $b \to u\ell\nu$, other $B\overline{B}$, and continuum backgrounds. These four types of events have distinct structures in the two-dimensional $m_{\rm ES}$–$\Delta E$ plane. We use the $m_{\rm ES}$–$\Delta E$ histograms obtained from the MC simulation as two-dimensional probability density functions (PDFs). The yields of the signal, $b \to u\ell\nu$ background and other $B\overline{B}$ background, subdivided in twelve, three and four $q^2$ bins, respectively, are extracted from a nineteen-parameter fit of the MC PDFs to the experimental data. The continuum background is corrected to match the off-resonance data control sample and is fixed in the fit. The number and type of fit parameters were chosen to provide a good balance between reliance on simulation predictions, complexity of the fit and total error size. $m_{\rm ES}$ and $\Delta E$ fit projections for the experimental data are shown in Fig. 1 in two ranges of $q^2$ corresponding to the sum of eight bins below and four bins above $q^2 = 16$ GeV$^2$. We obtain 5072±251 events for the total signal yield, $9867 \pm 564$ events for the $b \to u\ell\nu$ background, $33341 \pm 409$ events for the other $B\overline{B}$ backgrounds, and $9299 \pm 450$ events for the continuum yield. The fit has a $\chi^2$ value of 423 for 389 degrees of freedom.

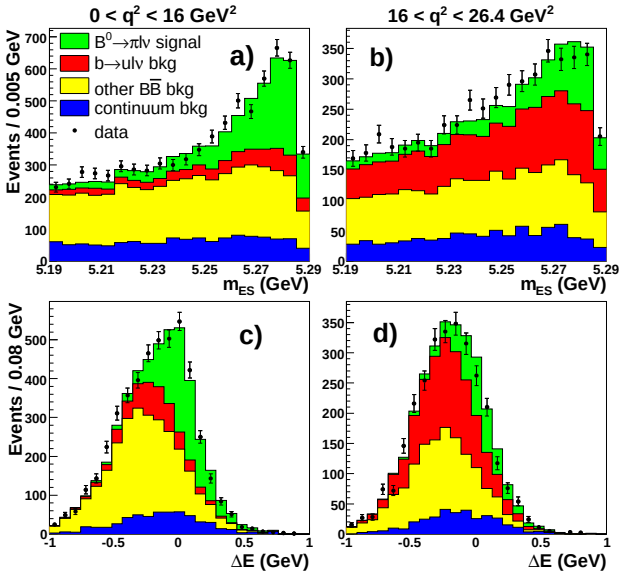


FIG. 1: Yield fit projections for (a,b) $m_{\rm ES}$ with $-0.16 < \Delta E < 0.20$ GeV; and (c,d) $\Delta E$ with $m_{\rm ES} > 5.272$ GeV. The distributions (a,c) are for $q^2 < 16$ GeV$^2$; and (b,d) are for $q^2 > 16$ GeV$^2$.

Numerous sources of systematic uncertainties and their correlations among the $q^2$ bins have been investigated. The uncertainties due to the detector simulation are established by varying within bounds given by control samples the tracking efficiency of all charged tracks, the particle identification efficiencies of signal candidate tracks, the calorimeter efficiency (varied separately for photons, $K^0_L$ and neutrons) and the energy deposited in the calorimeter by $K^0_L$ mesons. The reconstruction of these neutral particles affects the analysis via the neutrino reconstruction. The uncertainties due to the generator-level inputs to the simulation are established by varying, within errors [18], the BFs of the background processes $b \to u\ell\nu$, $b \to c\ell\nu$, $D \to X\ell\nu$ and $D \to K^0_L X$ as well as the BF of the $\Upsilon(4S) \to B^0\overline{B}^0$ decay. The $B^0 \to \pi^-\ell^+\nu$, $B \to \rho\ell\nu$, $B \to D\ell\nu$ and $B \to D^*\ell\nu$ form factors are varied within bounds given by recent calculations [19] or measurements [14, 18, 20]. The heavy quark parameters used in the simulation of non-resonant $b \to u\ell\nu$ events are varied according to Ref. [21]. We assign an uncertainty of 20% to the final state radiation (FSR) corrections calculated by PHOTOS [22, 23]. Finally, the uncertainties due to the modeling of the continuum are established by varying its $q^2$, $m_{\rm ES}$, and $\Delta E$ shapes and total yield within their errors given by comparisons with the off-resonance data control sample. The high statistics provided by our technique allow us to show that there is good agreement between data and simulation for the critical

TABLE I: Values of $\Delta\mathcal{B}(q^2)$ and their relative errors (%).

| $q^2$ bins ( GeV$^2$) | 4–6 | 16–18 | $q^2$<16 | $q^2$>16 | full $q^2$ range |
|---|---|---|---|---|---|
| BF ($10^{-4}$) | 0.16 | 0.13 | 1.09 | 0.38 | 1.46 |
| Fit error | 12.8 | 17.6 | 5.3 | 10.3 | 4.8 |
| Detector effects | 3.7 | 5.0 | 4.4 | 4.5 | 3.7 |
| Continuum bkg | 1.2 | 1.7 | 2.8 | 3.5 | 2.5 |
| $B \to X_u \ell\nu$ bkg | 3.0 | 3.1 | 2.3 | 4.7 | 2.5 |
| $B \to X_c \ell\nu$ bkg | 1.7 | 1.8 | 1.2 | 1.2 | 1.0 |
| Other effects | 3.4 | 3.0 | 2.3 | 2.3 | 2.3 |
| Total error | 14.2 | 19.0 | 8.2 | 12.9 | 7.5 |

variables in signal depleted, signal enhanced, $b \to u\ell\nu$ enhanced and continuum control samples. Consistent results are obtained either by dividing the final dataset into sub-samples or using modified binnings or modified event selections.

The partial BFs are calculated using the observed signal yields, the unfolding algorithm and the signal efficiencies given by the simulation. The total BF is given by the sum of the partial BFs, thereby reducing the sensitivity of the signal efficiency to the uncertainties of the $f_+(q^2)$ form factor. We compute the covariance matrix for each source of uncertainty and use these matrices to calculate the errors on the total BF. The fit and systematic errors are given in Table I for five ranges of $q^2$. The complete set of fit and systematic uncertainties of the partial and total BFs as well as their correlation matrices are given in Ref. [24]. Our value of the total BF, $(1.46 \pm 0.07_{stat} \pm 0.08_{syst}) \times 10^{-4}$, is comparable in precision to the world average prior to our result [18]: $(1.35 \pm 0.08_{stat} \pm 0.08_{syst}) \times 10^{-4}$. The systematic error is due in large part to the detector efficiency. The systematic errors arising from the BFs and form factors of the backgrounds have been reduced with respect to previous untagged measurements by the many-parameter fit to the background yields in the 12 bins of $q^2$.

The $\Delta\mathcal{B}(q^2)$ distribution is displayed in Fig. 2 together with theoretical predictions. We modify the measured $q^2$ distribution to remove FSR effects, in order to allow a direct comparison with the theoretical predictions which do not include such effects (this procedure is referred to as "No FSR" in Ref. [24]). We obtain the $f_+(q^2)$ shape from a fit to this distribution. The $\chi^2$ function minimized in the $f_+(q^2)$ fit uses a PDF based on the two-parameter BK parametrization. It is defined in terms of the $\Delta\mathcal{B}(q^2)$ covariance matrix to take into account the correlations among the measurements in the various $q^2$ bins. The fit gives $\alpha = 0.52 \pm 0.05_{stat} \pm 0.03_{syst}$, compared to our previous untagged measurement $\alpha = 0.61 \pm 0.09$ [8] (statistical error only) as well as a value of $|V_{ub} f_+(0)| = (9.6 \pm 0.3_{stat} \pm 0.2_{syst}) \times 10^{-4}$ from the fit extrapolated to $q^2 = 0$, with $P(\chi^2)$=65%. This value includes a 67%

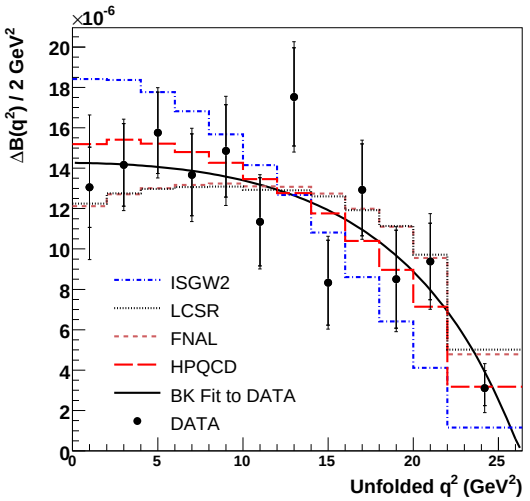


FIG. 2: Partial $\Delta\mathcal{B}(q^2)$ spectrum in 12 bins of $q^2$. The smaller error bars are statistical only while the larger ones also include systematic uncertainties. The solid black curve shows the result of the fit of the BK parametrization to the data. The data are also compared to unquenched LQCD calculations [3, 4], LCSR calculations [5], and the ISGW2 quark model [6].

TABLE II: Values of $|V_{ub}|$ derived from form-factor calculations. The first two errors arise from the statistical and systematic uncertainties of the partial BFs, respectively. The third error comes from the uncertainty on $\Delta\zeta$.

| | $q^2$ ( GeV$^2$) | $\Delta\zeta$ (ps$^{-1}$) | $\lvert V_{ub}\rvert$ ($10^{-3}$) |
|---|---|---|---|
| HPQCD [3] | > 16 | $1.46 \pm 0.35$ | $4.1 \pm 0.2 \pm 0.2\ ^{+0.6}_{-0.4}$ |
| FNAL [4] | > 16 | $1.83 \pm 0.50$ | $3.7 \pm 0.2 \pm 0.2\ ^{+0.6}_{-0.4}$ |
| LCSR [5] | < 16 | $5.44 \pm 1.43$ | $3.6 \pm 0.1 \pm 0.1\ ^{+0.6}_{-0.4}$ |
| ISGW2 [6] | 0–26.4 | $9.6 \pm 4.8$ | $3.2 \pm 0.1 \pm 0.1\ ^{+1.3}_{-0.6}$ |

anti-correlation between the shape and normalization parameters, $\alpha$ and $c_B$, and can be used to predict [25] rates of other decays such as $B \to \pi\pi$.

The $\chi^2$ probabilities have been calculated relative to the binned data result for various theoretical predictions, considering only experimental errors. We obtain $P(\chi^2)$=67% for HPQCD [3], 45% for FNAL [4] and 41% for LCSR [5]. The ISGW2 quark model [6], $P(\chi^2)$=0.06%, is clearly incompatible with our data.

We extract $|V_{ub}|$ from the partial BFs $\Delta\mathcal{B}(q^2)$ using the relation: $|V_{ub}| = \sqrt{\Delta\mathcal{B}(q^2)/(\tau_{B^0}\Delta\zeta)}$, where $\tau_{B^0} = 1.530 \pm 0.009$ ps [18] is the $B^0$ lifetime and $\Delta\zeta = \Gamma/|V_{ub}|^2$ is the normalized partial decay rate predicted by the form-factor calculations [3, 4, 5, 6]. Excluding the ISGW2 model, the values of $|V_{ub}|$ given in Table II range from $(3.6 - 4.1) \times 10^{-3}$.

In summary, we have measured the partial $B^0 \to \pi^-\ell^+\nu$ branching fractions in 12 bins of $q^2$ using a loose

neutrino reconstruction technique. We obtained the most precise measurement to date of the $\mathcal{B}(B^0 \to \pi^- \ell^+ \nu)$ and $|V_{ub} f_+(0)|$, as well as a detailed description of the $f_+(q^2)$ shape. This shape can be compared with various theoretical predictions and, in particular, shows that the ISGW2 model can be ruled out. From the most recently published unquenched LQCD calculation [3], we obtain $|V_{ub}| = \left(4.1 \pm 0.2_{stat} \pm 0.2_{syst}{}^{+0.6}_{-0.4\mathrm{FF}}\right) \times 10^{-3}$.

We are grateful for the excellent luminosity and machine conditions provided by our PEP-II colleagues, and for the substantial dedicated effort from the computing organizations that support *BABAR*. The collaborating institutions wish to thank SLAC for its support and kind hospitality. This work is supported by DOE and NSF (USA), NSERC (Canada), IHEP (China), CEA and CNRS-IN2P3 (France), BMBF and DFG (Germany), INFN (Italy), FOM (The Netherlands), NFR (Norway), MIST (Russia), MEC (Spain), and PPARC (United Kingdom). Individuals have received support from the Marie Curie EIF (European Union) and the A. P. Sloan Foundation.

* Deceased
† Also with Università di Perugia, Dipartimento di Fisica, Perugia, Italy
‡ Also with Università della Basilicata, Potenza, Italy
§ Also with IPPP, Physics Department, Durham University, Durham DH1 3LE, United Kingdom

[1] M. Kobayashi and T. Maskawa, Prog. Theor. Phys. **49**, 652 (1973).
[2] Charge conjugate decays and $\ell = e$ or $\mu$ are implied throughout this paper.
[3] E. Gulez *et al.* (HPQCD Collaboration), Phys. Rev. **D73**, 074502 (2006).
[4] M. Okamoto *et al.*, Nucl. Phys. Proc. Suppl. **140**, 461 (2005).
[5] P. Ball and R. Zwicky, Phys. Rev. **D71**, 014015 (2005).
[6] D. Scora and N. Isgur, Phys. Rev. **D52**, 2783 (1995).
[7] S. B. Athar *et al.* (CLEO Collaboration), Phys. Rev. **D68**, 072003 (2003).
[8] B. Aubert *et al.* (*BABAR* Collaboration), Phys. Rev. **D72**, 051102 (2005).
[9] B. Aubert *et al.* (*BABAR* Collaboration), Phys. Rev. Lett. **97**, 211801 (2006).
[10] T. Hokuue *et al.* (Belle Collaboration), hep-ex/0604024, submitted to Phys. Lett. B.
[11] B. Aubert *et al.* (*BABAR* Collaboration), Nucl. Instrum. Methods **A479**, 1 (2002).
[12] D. Côté *et al.*, Eur. Phys. J. C **38**, 105 (2004).
[13] D. Becirevic and A. B. Kaidalov, Phys. Lett. **B478**, 417 (2000).
[14] B. Aubert *et al.* (*BABAR* Collaboration), Phys. Rev. **D74**, 092004 (2006).
[15] G. Cowan, Statistical Data Analysis, Chap. 11, Oxford University Press (1998).
[16] B. Aubert *et al.* (*BABAR* Collaboration), Phys. Rev. **D67**, 031101 (2003).
[17] R.J. Barlow and C. Beeston, Comput. Phys. Commun. **77**, 219 (1993).
[18] W.-M. Yao *et al.* (Particle Data Group), J. Phys. **G33**, 1 (2006).
[19] P. Ball and R. Zwicky, Phys. Rev. **D71**, 014029 (2005).
[20] B. Aubert *et al.* (*BABAR* Collaboration), hep-ex/0607060.
[21] O. L. Buchmüller and H. U. Flächer, Phys. Rev. **D73**, 073008 (2006).
[22] E. Barberio and Z. Was, Comput. Phys. Commun. **79**, 291 (1994).
[23] E. Richter-Was *et al.*, Phys. Lett. **B303**, 163 (1993).
[24] See EPAPS Document No. *xxxxxx* for tables of systematic errors and error matrices. For more information on EPAPS, see http://www.aip.org/pubservs/epaps.html.
[25] T. Becher and R. J. Hill, Phys. Lett. **B633**, 61 (2006).

## Electronic Physics Auxiliary Publication Service (EPAPS)

This is an EPAPS attachment to B. Aubert *et al.* (*BABAR* Collaboration), *BABAR*-PUB-06/069, SLAC-PUB-12253, hep-ex/0612020, submitted to Phys. Rev. Lett. For more information on EPAPS, see http://www.aip.org/pubservs/epaps.html.

TABLE A-1: $B^0 \to \pi^-\ell^+\nu$ yields, efficiency (%), $\Delta\mathcal{B}$ ($10^{-7}$) and their relative errors (%). The $\Delta\mathcal{B}$ and efficiency values labelled "No FSR" are modified to remove FSR effects. This procedure has no significant impact on the $\Delta\mathcal{B}$ values.

| $q^2$ bins ( GeV$^2$) | 0-2 | 2-4 | 4-6 | 6-8 | 8-10 | 10-12 | 12-14 | 14-16 | 16-18 | 18-20 | 20-22 | 22-26.4 | $q^2$<16 | $q^2$>16 | Total |
|---|---|---|---|---|---|---|---|---|---|---|---|---|---|---|---|
| Fitted yield | 366.6 | 462.9 | 499.5 | 451.8 | 436.4 | 391.0 | 522.7 | 333.6 | 458.0 | 355.4 | 364.8 | 428.8 | 3464.6 | 1606.9 | 5071.5 |
| Fit error | 12.9 | 9.7 | 8.6 | 9.7 | 11.2 | 13.0 | 11.7 | 17.4 | 15.6 | 21.7 | 15.9 | 17.3 | 5.3 | 9.9 | 5.0 |
| Systematic error | 20.0 | 6.3 | 3.2 | 4.9 | 6.3 | 4.1 | 4.3 | 6.1 | 4.9 | 7.9 | 12.3 | 17.4 | 3.7 | 7.3 | 3.9 |
| Unfolded yield | 374.7 | 452.3 | 515.3 | 442.2 | 459.1 | 360.7 | 583.4 | 302.7 | 514.3 | 357.7 | 406.3 | 303.0 | 3490.2 | 1581.3 | 5071.5 |
| Fit error | 15.2 | 14.4 | 12.8 | 14.8 | 15.4 | 19.2 | 13.9 | 25.2 | 17.6 | 28.5 | 20.2 | 27.7 | 5.4 | 10.2 | 5.0 |
| Systematic error | 22.9 | 7.3 | 3.7 | 5.6 | 7.8 | 5.2 | 4.8 | 8.9 | 5.2 | 10.0 | 14.9 | 27.3 | 3.7 | 7.6 | 3.9 |
| Efficiency | 6.56 | 7.13 | 7.22 | 7.11 | 6.76 | 6.97 | 7.21 | 7.87 | 8.68 | 9.20 | 9.37 | 9.66 | - | - | - |
| Eff. (No FSR) | 6.31 | 7.02 | 7.19 | 7.11 | 6.79 | 6.99 | 7.32 | 7.99 | 8.75 | 9.25 | 9.53 | 9.73 | - | - | - |
| $\Delta\mathcal{B}$ | 125.5 | 139.5 | 156.9 | 136.8 | 149.4 | 113.7 | 177.9 | 84.5 | 130.3 | 85.5 | 95.3 | 68.9 | 1084.3 | 380.0 | 1464.3 |
| $\Delta\mathcal{B}$ (No FSR) | 130.6 | 141.6 | 157.5 | 136.7 | 148.6 | 113.5 | 175.3 | 83.3 | 129.3 | 85.1 | 93.8 | 68.4 | 1087.1 | 376.6 | 1463.7 |
| Fit error | 15.2 | 14.4 | 12.8 | 14.8 | 15.4 | 19.2 | 13.9 | 25.2 | 17.6 | 28.5 | 20.2 | 27.7 | 5.3 | 10.3 | 4.8 |
| Systematic error | 23.7 | 7.0 | 6.2 | 8.1 | 9.6 | 7.3 | 7.1 | 11.0 | 7.0 | 11.0 | 14.9 | 27.0 | 6.3 | 7.8 | 5.7 |

TABLE A-2: Relative errors (%) of the partial and total $\mathcal{B}(B^0 \to \pi^-\ell^+\nu)$ from all sources. FSR effects are included.

| $q^2$ bins ( GeV$^2$) | 0-2 | 2-4 | 4-6 | 6-8 | 8-10 | 10-12 | 12-14 | 14-16 | 16-18 | 18-20 | 20-22 | 22-26.4 | $q^2$<16 | $q^2$>16 | Total |
|---|---|---|---|---|---|---|---|---|---|---|---|---|---|---|---|
| Tracking efficiency | 1.6 | 1.7 | 1.3 | 3.1 | 3.8 | 1.3 | 1.8 | 7.1 | 2.3 | 1.7 | 2.2 | 9.2 | 1.9 | 1.8 | 1.1 |
| $\gamma$ efficiency | 4.7 | 1.3 | 2.6 | 5.0 | 3.6 | 3.2 | 3.5 | 3.1 | 3.0 | 3.5 | 3.8 | 7.0 | 2.9 | 1.7 | 1.9 |
| $K^0_L$ & neutrons | 0.7 | 0.6 | 0.7 | 1.0 | 1.2 | 1.2 | 1.2 | 1.3 | 2.0 | 1.5 | 1.1 | 2.2 | 0.5 | 1.0 | 0.6 |
| Particle ID | 7.0 | 2.5 | 2.1 | 1.9 | 0.7 | 2.7 | 2.6 | 2.5 | 2.6 | 3.4 | 2.9 | 7.0 | 2.6 | 3.6 | 2.9 |
| Continuum yield | 7.0 | 0.5 | 0.6 | 0.2 | 0.9 | 1.0 | 0.6 | 0.8 | 0.6 | 1.9 | 1.1 | 4.0 | 1.0 | 1.6 | 1.0 |
| Continuum $q^2$ | 20.1 | 1.5 | 1.0 | 1.0 | 1.7 | 1.8 | 1.5 | 2.0 | 1.5 | 3.3 | 4.0 | 8.7 | 2.4 | 1.9 | 1.8 |
| Continuum $m_{\rm ES}$ | 1.1 | 0.3 | 0.1 | 0.1 | 0.1 | 0.1 | 0.3 | 0.6 | 0.3 | 0.6 | 0.7 | 1.0 | 0.2 | 0.5 | 0.2 |
| Continuum $\Delta E$ | 3.0 | 1.6 | 0.5 | 1.0 | 1.5 | 0.2 | 0.1 | 1.2 | 0.6 | 1.8 | 3.8 | 5.2 | 1.0 | 2.5 | 1.4 |
| $B \to X_u\ell\nu$ BFs | 1.2 | 1.4 | 0.7 | 0.7 | 1.0 | 1.4 | 1.1 | 1.8 | 1.7 | 3.6 | 10.4 | 12.1 | 0.9 | 3.4 | 1.2 |
| SF param | 0.4 | 0.5 | 0.3 | 0.5 | 0.1 | 0.1 | 0.1 | 0.4 | 0.4 | 4.1 | 5.7 | 14.9 | 0.2 | 2.1 | 0.7 |
| $B \to \rho\ell\nu$ FFs | 1.3 | 0.7 | 1.8 | 1.1 | 0.8 | 1.1 | 1.2 | 3.2 | 0.5 | 3.3 | 1.3 | 4.3 | 0.9 | 0.8 | 0.6 |
| $B^0 \to \pi^-\ell^+\nu$ FF | 0.4 | 0.5 | 0.5 | 0.5 | 0.5 | 0.5 | 0.5 | 0.8 | 0.7 | 0.7 | 1.1 | 3.5 | 0.5 | 1.3 | 0.7 |
| FSR | 0.7 | 1.5 | 2.2 | 1.9 | 2.6 | 2.7 | 2.2 | 0.6 | 2.5 | 2.0 | 1.3 | 1.1 | 1.9 | 1.8 | 1.9 |
| $B \to X_c\ell\nu$ BFs | 1.8 | 2.1 | 1.1 | 2.2 | 4.6 | 1.2 | 2.4 | 2.2 | 1.3 | 2.5 | 1.7 | 2.2 | 0.9 | 1.0 | 0.8 |
| $B \to D^*\ell\nu$ FFs | 0.7 | 1.1 | 0.1 | 1.6 | 3.1 | 0.8 | 1.4 | 1.0 | 0.9 | 1.2 | 0.6 | 2.7 | 0.7 | 0.4 | 0.6 |
| $B \to D\ell\nu$ FF | 1.7 | 1.2 | 0.7 | 0.3 | 2.2 | 0.4 | 0.1 | 0.7 | 0.6 | 0.9 | 0.4 | 0.7 | 0.1 | 0.4 | 0.2 |
| $\Upsilon(4S) \to B^0\overline{B}^0$ BF | 2.1 | 2.5 | 1.5 | 1.5 | 1.3 | 1.7 | 1.6 | 1.2 | 1.6 | 1.0 | 2.4 | 1.9 | 1.7 | 1.7 | 1.7 |
| $D \to X\ell\nu$ BFs | 2.3 | 2.8 | 1.1 | 1.3 | 1.6 | 1.1 | 1.1 | 0.9 | 0.6 | 0.9 | 1.0 | 0.8 | 0.4 | 0.5 | 0.3 |
| $D \to K^0_L$ BFs | 0.6 | 1.7 | 2.3 | 1.5 | 2.0 | 2.3 | 1.0 | 4.2 | 1.8 | 3.9 | 1.0 | 1.7 | 1.1 | 1.0 | 1.1 |
| B counting | 1.1 | 1.1 | 1.1 | 1.1 | 1.1 | 1.1 | 1.1 | 1.1 | 1.1 | 1.1 | 1.1 | 1.1 | 1.1 | 1.1 | 1.1 |
| Signal MC stat error | 1.5 | 1.7 | 1.6 | 1.9 | 1.6 | 1.9 | 1.4 | 1.8 | 1.4 | 1.6 | 1.3 | 1.5 | 0.5 | 0.6 | 0.4 |
| Total systematic error | 23.7 | 7.0 | 6.2 | 8.1 | 9.6 | 7.3 | 7.1 | 11.0 | 7.0 | 11.0 | 14.9 | 27.0 | 6.3 | 7.8 | 5.7 |
| Fit error | 15.2 | 14.4 | 12.8 | 14.8 | 15.4 | 19.2 | 13.9 | 25.2 | 17.6 | 28.5 | 20.2 | 27.7 | 5.3 | 10.3 | 4.8 |
| Total error | 28.2 | 16.1 | 14.2 | 16.9 | 18.2 | 20.5 | 15.6 | 27.5 | 19.0 | 30.6 | 25.1 | 38.7 | 8.2 | 12.9 | 7.5 |

TABLE A-3: Correlation matrix of the partial $\Delta\mathcal{B}(B^0 \to \pi^-\ell^+\nu, q^2)$ statistical errors. The correlations have the same values for the "No FSR" case as for the one with FSR, within the quoted precision.

| $q^2$ bins ($\mathrm{GeV}^2$) | 0-2 | 2-4 | 4-6 | 6-8 | 8-10 | 10-12 | 12-14 | 14-16 | 16-18 | 18-20 | 20-22 | 22-26.4 |
|---|---|---|---|---|---|---|---|---|---|---|---|---|
| 0-2 | 1.00 | -0.26 | 0.11 | 0.01 | 0.06 | 0.01 | 0.03 | -0.01 | -0.00 | -0.00 | -0.00 | -0.01 |
| 2-4 | -0.26 | 1.00 | -0.33 | 0.14 | 0.03 | -0.00 | 0.01 | -0.00 | -0.00 | -0.00 | -0.00 | -0.00 |
| 4-6 | 0.11 | -0.33 | 1.00 | -0.30 | 0.21 | 0.05 | 0.13 | -0.02 | -0.00 | -0.00 | -0.00 | -0.00 |
| 6-8 | 0.01 | 0.14 | -0.30 | 1.00 | -0.22 | 0.15 | 0.09 | -0.01 | -0.00 | -0.00 | -0.00 | -0.00 |
| 8-10 | 0.06 | 0.03 | 0.21 | -0.22 | 1.00 | -0.22 | 0.20 | -0.03 | 0.00 | -0.00 | -0.00 | -0.00 |
| 10-12 | 0.01 | -0.00 | 0.05 | 0.15 | -0.22 | 1.00 | -0.02 | 0.02 | -0.00 | 0.00 | -0.00 | -0.00 |
| 12-14 | 0.03 | 0.01 | 0.13 | 0.09 | 0.20 | -0.02 | 1.00 | -0.25 | -0.00 | -0.03 | 0.00 | -0.00 |
| 14-16 | -0.01 | -0.00 | -0.02 | -0.01 | -0.03 | 0.02 | -0.25 | 1.00 | 0.06 | 0.21 | -0.06 | -0.04 |
| 16-18 | -0.00 | -0.00 | -0.00 | -0.00 | 0.00 | -0.00 | -0.00 | 0.06 | 1.00 | 0.13 | -0.08 | -0.06 |
| 18-20 | -0.00 | -0.00 | -0.00 | -0.00 | -0.00 | 0.00 | -0.03 | 0.21 | 0.13 | 1.00 | -0.21 | -0.13 |
| 20-22 | -0.00 | -0.00 | -0.00 | -0.00 | -0.00 | -0.00 | 0.00 | -0.06 | -0.08 | -0.21 | 1.00 | -0.05 |
| 22-26.4 | -0.01 | -0.00 | -0.00 | -0.00 | -0.00 | -0.00 | -0.00 | -0.04 | -0.06 | -0.13 | -0.05 | 1.00 |

TABLE A-4: Correlation matrix of the partial $\Delta\mathcal{B}(B^0 \to \pi^-\ell^+\nu, q^2)$ systematic errors. The correlations have the same values for the "No FSR" case as for the one with FSR, within the quoted precision.

| $q^2$ bins ($\mathrm{GeV}^2$) | 0-2 | 2-4 | 4-6 | 6-8 | 8-10 | 10-12 | 12-14 | 14-16 | 16-18 | 18-20 | 20-22 | 22-26.4 |
|---|---|---|---|---|---|---|---|---|---|---|---|---|
| 0-2 | 1.00 | 0.19 | 0.32 | 0.11 | -0.06 | 0.46 | 0.44 | 0.13 | 0.31 | 0.23 | 0.13 | 0.00 |
| 2-4 | 0.19 | 1.00 | 0.21 | -0.09 | -0.28 | 0.31 | 0.11 | -0.05 | 0.23 | 0.14 | 0.18 | 0.35 |
| 4-6 | 0.32 | 0.21 | 1.00 | 0.66 | 0.46 | 0.74 | 0.58 | 0.52 | 0.56 | 0.30 | 0.04 | 0.04 |
| 6-8 | 0.11 | -0.09 | 0.66 | 1.00 | 0.75 | 0.58 | 0.67 | 0.60 | 0.54 | 0.27 | -0.05 | -0.09 |
| 8-10 | -0.06 | -0.28 | 0.46 | 0.75 | 1.00 | 0.32 | 0.59 | 0.48 | 0.35 | 0.13 | 0.04 | -0.11 |
| 10-12 | 0.46 | 0.31 | 0.74 | 0.58 | 0.32 | 1.00 | 0.67 | 0.37 | 0.55 | 0.36 | 0.08 | 0.05 |
| 12-14 | 0.44 | 0.11 | 0.58 | 0.67 | 0.59 | 0.67 | 1.00 | 0.32 | 0.62 | 0.36 | 0.08 | -0.14 |
| 14-16 | 0.13 | -0.05 | 0.52 | 0.60 | 0.48 | 0.37 | 0.32 | 1.00 | 0.40 | 0.28 | 0.05 | -0.11 |
| 16-18 | 0.31 | 0.23 | 0.56 | 0.54 | 0.35 | 0.55 | 0.62 | 0.40 | 1.00 | 0.54 | 0.05 | -0.08 |
| 18-20 | 0.23 | 0.14 | 0.30 | 0.27 | 0.13 | 0.36 | 0.36 | 0.28 | 0.54 | 1.00 | -0.10 | 0.23 |
| 20-22 | 0.13 | 0.18 | 0.04 | -0.05 | 0.04 | 0.08 | 0.08 | 0.05 | 0.05 | -0.10 | 1.00 | 0.08 |
| 22-26.4 | 0.00 | 0.35 | 0.04 | -0.09 | -0.11 | 0.05 | -0.14 | -0.11 | -0.08 | 0.23 | 0.08 | 1.00 |